Distributed Attitude Synchronization Control of Switched Networked Satellite Formation Flying

Belkacem Kada (bkada@kau.edu.sa)
King Abdulaziz University https://orcid.org/0000-0002-1087-6634

Research Article

Keywords: Distributed consensus, satellite formation flying, multi-agent systems, high-order sliding mode

Posted Date: February 21st, 2022

DOI: https://doi.org/10.21203/rs.3.rs-1349545/v1

Distributed Attitude Synchronization Control of Switched Networked Satellite Formation Flying

Belkacem Kada *[1], Ahmed. ALzubairi[1]

[1]*Department of Aeronautical and Aerospace Engineering, King Abdulaziz University, Jeddah, Saudi Arabia,*

** bkada@kau.edu.sa*

Abstract: This paper addresses the leader-follower finite-time attitude synchronization and stabilization for satellite formation flying (SFF) under directed switching communication topologies. Specifically, a distributed attitude synchronization control scheme is proposed to guarantee finite-time convergence to leader's attitude and desired angular velocity for SFF under time-varying but jointly connected switching communication topologies. First, finite-time consensus protocols are designed for leader's attitude tracking. The protocols are developed based on non-smooth control techniques such as homogeneity with dilatation and LaSalle invariance principle. Then, a distributed finite-time angular velocity estimator is designed using super-twisting sliding-mode control. The estimator helps solving communication loss issues, reducing communication burden, and canceling chattering effect due to high-rate convergence. Simulations are shown to illustrate the effectiveness of the obtained theoretical results.

Keywords: Distributed consensus, satellite formation flying, multi-agent systems, high-order sliding mode

1. Introduction

The decentralized coordinated attitude control for Satellite Formation Flying (SFF) consists one of the main technical requirements for the success of SFF missions. The main challenge to maintain formation attitude alignment is the synchronization convergence rate.

The convergence speed of SFF synchronization consists one of the most important aspects of SFF control and stabilization. A high convergence rate is strongly recommended for high-accuracy, robust, and low-energy synchronization. In other words, the effectiveness of a synchronization algorithm is measured by its convergence time. Over the last decades, a variety of SFF attitude synchronization algorithms has been developed to satisfy SFF attitude synchronization requirements [1-10]. However, most existing results only show asymptotic convergence, which is slow and high-energy consuming.

To accelerate the SFF synchronization convergence rate and improve SFF robustness, finite-time attitude alignment has recently drawn the attention of SFF researchers as one of the promising solutions. Zhou and Hu [11] designed a SFF decentralized finite-time attitude synchronization controller and an angular speed estimator using first-order sliding mode. Liu et al. [12] addressed the problem of SFF attitude coordination in the presence of disturbances and noises based on the reference attitude trajectory. The authors combined reference model control, H_∞ method, sliding mode control, and linear matrix inequality method to ensure global robust attitude tracking and formation keeping. Integral sliding mode control was used in [13] to design adaptive attitude coordinated tracking protocols for a group of rigid spacecrafts. Authors designed the control system to handle formation control problems such as parameters uncertainties, external disturbances, and input saturations. A robust SFF control system was proposed by Liu et al. [14] for trajectory and attitude control to form the desired formation and align the satellite attitudes. Output feedback control was used in [15] to design a law for finite-time attitude synchronization of spacecraft formation flying. The control law was developed combining homogenous system theory with a nonlinear filter to avoid angular velocity measurement. The control scheme provided the attitude synchronization with zero final angular velocity. In [16], authors combined a distributed continuous protocol with an adaptive sliding mode observer to ensure finite-time synchronization of spacecraft formation without velocity measurement. Nonsingular fast terminal sliding mode was used in [17] to design a decentralized adaptive control law for attitude synchronization of a group of spacecrafts. On the other hand, inter-satellite communications (ISC) in autonomous SFF is a key aspect of promoting on-orbit activities such as autonomous data transfer, distributed processing, and proximity operations. ISC enable individual satellites to share navigation and control information. Exchanging attitude and position formation among satellites fosters SFF stability and synchronization. However, the dynamic change of SFF communication topology and loss of communication make the design of distributed consensus and formation protocols very challenging problem.

Very few investigations have been studying the problem of finite-time time-varying SFF synchronization and stabilization. In [18], the problem of attitude synchronization for spacecraft formation in dynamic environments has been addressed. The authors proposed an adaptive control scheme that can ensure attitude synchronization with switching communication topologies at asymptotic rate of convergence. The proposed tracking control method requires that the switching topologies be jointly connected in finite-time intervals. However, according to the obtained results, it is observed that the convergence of the method is slow. Authors in [19] proposed another control scheme to remedy the problem of attitude synchronization in the absence of angular velocity information and under switching topologies. The control scheme was developed combining auto-stable region and Lyapunov function approaches. Although the simulation results show fast convergence, the required control torques exhibit a chattering-like effect with high amplitude. Nonlinear fast terminal sliding mode control was combined with adaptive fuzzy control in [20] to design a distributed finite-time control algorithm for a team of spacecraft vehicles. Although the algorithm guarantees finite-time convergence of spacecraft formation under switching topologies, it presents high overshooting of angular speed tracking and sliding mode chattering effect. In [20], the attitude synchronization problem of switched networked spacecraft systems has been tackled within leader-following based formations. A distributed control law was developed based on asymptotic convergence analysis and using lemmas about exponential convergence, stability of switched systems, certainly equivalence principal control, and asymptotic distributed observation. An event-triggered based coordinated control of SFF under limited communication has been proposed in [22]. By cancelling the continuous neighbor-to-neighbor velocity exchange, the coordinated controller conjointly with the event-triggered mechanism reduced the communication burden and the computational cost. Nevertheless, the simulation results reveal that the convergence time of the event-triggered controller is relatively long, and the control signals suffer from chattering effect, which can damage the actuation system of the individual spacecraft. A high-order sliding mode-based spacecraft formation control scheme was proposed in [23]. In this contribution, the super-twisting sliding mode control has been used to design a distributed observer and sufficient conditions for time-varying practical formation have been developed in term of average dwell time. Although, the proposed algorithm has shown good tracking, no indication was given about the control efforts magnitude and their vulnerability to chattering.

Motivated by the above results, this paper addresses the finite-time distributed control design for SFF systems subject to loss of communication. Specifically, our main contribution is the development of a robust distributed control scheme that would enable satellite system networks to achieve consensus and formation objectives in leader-follower switching topology architecture with fast rate convergence and chattering free control. The control scheme consists of a distributed formation synchronization controller and an angular velocity estimator. The distributed control law is developed using leader-follower consensus approach for undirected communication topologies and the estimator is designed using high-order sliding mode control.

The first part of the paper studies the finite-time distributed attitude synchronization problem of SFF under fixed and switched communication topologies. The theoretical aspect of the SFF consensus is investigated based on the graph theory, Lyapunov's direct method, homogeneity with dilation, and LaSalle's invariance principle. In the second part, and to maintain the SFF in case of communication loss between agents or with the leader, a distributed second order sliding mode observer based on the super-twisting algorithm is designed. Conjointly with the attitude synchronization controller, the observer allows the individual satellites to estimate the desired angular velocity in case of ISC links break. The super-twisting sliding mode control ensures the finite-time convergence of the sliding surface, cancels or alleviates the chattering effect of conventional sliding mode, and provides robustness against parameter uncertainties.

The rest of the paper is organized as follows. In section 2, satellite attitude kinematics and dynamics are formulated using quaternions, the basics of graph theory are given, and the necessary assumption and lemmas are made. Section 3 presents the main results of this work about the distributed SFF synchronization control protocols under undirected fixed and switched communication topologies. Section 4 presents the design of the distributed finite-time super-twisting estimator for individual satellites to obtain an accurate estimation of the leader angular velocity in case of break of ISC links or loss of communication with the leader. The effectiveness of the proposed control scheme is validated via numerical simulations in section 5. Finally, conclusions are made in section 6.

2. Preliminaries

Consider the case of a group of N satellites in a SFF and use subscribe $i \in \mathcal{N} = \{1,2,\dots,N\}$ to denote the ith agent satellite. The following preliminaries are given to solve the finite-time attitude synchronization problem of SFF.

2.1 Satellite attitude kinematics and dynamics

Let $\mathcal{F}_0$, $\mathcal{F}_\mathrm{i}$, $\mathcal{F}_\mathrm{F}$ being the inertial, satellite body, and formation frames, respectively. Consider the quaternion $\overline{\boldsymbol{q}}_i = [q_{0i} \quad \boldsymbol{q}_i]^T$ and the vector $\boldsymbol{\omega}_\mathrm{i}$ to denote the orientation and the angular velocity of the ith satellite from the frame $\mathcal{F}_\mathrm{i}$ to the frame $\mathcal{F}_0$, respectively. $\boldsymbol{q}_i$ and $\mathrm{q}_{0\mathrm{i}}$ are the vector part and scaler part of the quaternion and $\overline{\boldsymbol{q}}_i^* = [\pm q_{0i} \quad -\boldsymbol{q}_i]^T$ denotes the inverse of the quaternion. The rigid-body kinematics and dynamics of the ith satellite from the frame $\mathcal{F}_\mathrm{i}$ to the frame $\mathcal{F}_0$ can be described as follows [24]

$$\begin{aligned}
\dot{\boldsymbol{q}}_i &= -\frac{1}{2}\boldsymbol{\omega}_i^\times \times \boldsymbol{q}_i + \frac{1}{2} q_{0i}\,\boldsymbol{\omega}_i \\
\dot{q}_{0i} &= -\frac{1}{2}\,\boldsymbol{\omega}_i^T \boldsymbol{q}_i \\
\boldsymbol{J}_i \dot{\boldsymbol{\omega}}_i &= -\boldsymbol{\omega}_i^\times (J_i \boldsymbol{\omega}_i) + \boldsymbol{\tau}_i + \boldsymbol{d}_i
\end{aligned} \tag{1}$$

where $\mathbf{J}_\mathrm{i} \in \mathrm{R}^{3\times3}$, $\boldsymbol{\tau}_\mathrm{i} =\in \mathrm{R}^{3\times1}$, and $\boldsymbol{d}_\mathrm{i} =\in \mathrm{R}^{3\times1}$ denote the inertia tensor, the control vector of torques, and the external disturbance torque of the ith satellite, respectively.

2.2 Graph theory

Define $G = \{\mathcal{V}, \mathcal{E}, \boldsymbol{\mathcal{A}}\}$ as the weighted graph that describes the communication topology among the SFF agents. $\mathcal{V} = \{v_1, v_2, \dots, v_N\}$ denotes the nonempty set of the N nodes (satellites) and $\mathcal{E} \subseteq \mathcal{V} \times \mathcal{V}$ denotes the edge set (ISC links). The weighted adjacency matrix $\boldsymbol{\mathcal{A}} \in R^{n,n}$ is defined with nonnegative adjacency elements $a_{ij} \geq 0, \forall\, i,j \in \mathcal{N}$. The communication topology described by the graph G is supposed to fulfil the following properties:

- An edge $e_{ij} = (v_1, v_2) \in \mathcal{E}$ indicates the communication link from the ith satellite (parent) to the jth satellite (child).
- If $e_{ij} \in \mathcal{E}$ then $a_{ij} > 0$ else $a_{ij} = 0$.

- If the graph G is indirect where the satellites exchange information with each other then $a_{ij} = a_{ji} > 0$.
- $\forall\ (i, i) \in \mathcal{E}$, $a_{ii} = 0$ (i.e., the graph G has no self-loops).
- It corresponds to the graph G a Laplacian matrix $\boldsymbol{L}[l_{ij}] \in \mathbb{R}^{n,n}$

$$l_{ij} = \begin{cases} -a_{ij} & if \quad i \neq j \\ -\sum_{j=1, j\neq i}^{N} l_{ij} & if \quad i = j \end{cases} \tag{2}$$

2.3 Assumptions and lemmas

Assumption 1: In the leader-follower SFF considered in this paper, the vertex v_d represents the leader while the vertices $v_1, v_2, \dots, v_N$ represent the followers.
Assumption 2: Only one or few followers communicate with the leader. If a follower satellite 'i' is connected to the leader, then the connection weight is denoted by $b_i > 0$, otherwise $b_i = 0, \forall\ i \in \mathcal{N}$.
Assumption 3: The states of all followers can be affected directly or indirectly by the leader states under a set of protocols $\boldsymbol{\tau}_i$ satisfying $b_i \geq 0$.
Assumption 4: the switched graph G_s is undirected and connected in each interval $[t_k, t_{k+1})$.
Lemma 1 [25,26]: If the graph G is indirect and connected then the Laplacian matrix $\boldsymbol{L}$ is semi-positive definite, its eigenvalues are real and satisfy $0 = \lambda_1(\boldsymbol{L}) < \lambda_2(\boldsymbol{L}) \leq \cdots \lambda_N(\boldsymbol{L})$, with $\mathbf{1}_N = [1,1, \dots, 1]^T$ is a right eigenvector to $\lambda_1(\boldsymbol{L})$.
Lemma 2 [27,28] (Non-smooth LaSalle Invariance Principle): Consider the nonlinear dynamical system $\dot{\boldsymbol{x}} = \boldsymbol{f}(\boldsymbol{x}), \boldsymbol{f}(0) = 0$ with $\boldsymbol{x}(0) = \boldsymbol{x}_0$ and $\boldsymbol{f}: \boldsymbol{D} \to \mathbb{R}^n$ is a locally Lipchitz function defined over an open subset $\boldsymbol{D} \subset \mathbb{R}^n$ $(0 \in \boldsymbol{D})$. Let $\boldsymbol{\Omega} \subset \boldsymbol{D}$ be a positively invariant compact set of $\mathbf{D}$, $\mathrm{V}(\boldsymbol{x}): \boldsymbol{D} \to \mathbb{R}$ be a continuously differentiable positive definite function over $\boldsymbol{D}$ such that $D^+ V(\boldsymbol{x}) \leq 0$ in $\boldsymbol{\Omega}$, and $\boldsymbol{S} = \{\boldsymbol{x} \in \boldsymbol{\Omega} \mid D^+ V(\boldsymbol{x}) = 0\}$ whereD^+ denote the upper Dini derivative. Then the positive limit $L^+(\boldsymbol{x}_0)$ set is a compact nonempty invariant set.
Lemma 3 [29] (Finite-time convergence in homogeneous systems): Suppose that the vector field of the system $\dot{\boldsymbol{x}} = \boldsymbol{f}(\boldsymbol{x})$ is continuous and homogenous of degree p with dilation coefficient $r = (r_1, r_2, \dots, r_n), r_i > 0, i = 1,2, \dots, n$. Then

- If $p > 0$, $x = 0$ is an asymptotically stable equilibrium of the system.
- If $p = 0$, the system equilibrium is exponentially stable.
- If $p < 0$, the system equilibrium is locally finite-time stable

It results from Lemma 3 that there exists a C^m-smooth homogeneous Lyapunov function $\mathrm{V}(\boldsymbol{x}): \boldsymbol{D} \to \mathbb{R}$ of degree of homogeneity $l > 0$ where for any $\varepsilon > 0$

$$V(\varepsilon^{r_1} x_1, \dots, \varepsilon^{r_n} x_n) = \varepsilon^l V(x_1, \dots, x_n) \tag{3}$$

For the case $p < 0$, the following condition holds when $t \leq -p/(ck)\, V_0^{t/l}$

$$V(t) \leq \left(c_1 \frac{k}{p} t + V_0^{-\frac{1}{l}}\right)^{-\frac{1}{l}} \tag{4}$$

where V_0 is an initial value of V and for $\|w\|_{\{r,2\}} = 1$ (homogeneous norm)

$$c_1 = \sup_{w \in \{y \mid \|y\|_{\{r,2\}} = 1\}} \frac{\langle \nabla V(w). \boldsymbol{F}(w) \rangle}{\nabla V(w)^{\frac{l+1}{l}}} \tag{5}$$

For $t_1 = -p/(ck)\, V_0^{t/l}$, $V(t_1) = 0$ and

$$V(t) = 0 \qquad (t > t_2) \tag{6}$$

This proves the finite-time stability of the homogenous system $\dot{\boldsymbol{x}} = \boldsymbol{f}(\boldsymbol{x})$.
Lemma 4 [30] (Local finite-time convergence in homogeneous systems): Suppose Lemma 3 holds, if $\tilde{\boldsymbol{f}}$ is a continuous vector field satisfying

$$\dot{\boldsymbol{x}} = \boldsymbol{f}(\boldsymbol{x}) + \tilde{\boldsymbol{f}}(\boldsymbol{x}), \qquad \tilde{\boldsymbol{f}}(\mathbf{0}) = \mathbf{0},\ \boldsymbol{x} \in \mathbb{R}^n \tag{7}$$

and

$$\lim_{\varepsilon \to 0} \frac{\tilde{f}_i(\varepsilon^{r_1} x_1, \dots, \varepsilon^{r_n} x_n)}{\varepsilon^{r_1 + l}} = 0, \quad \forall \boldsymbol{x} \neq 0, i = 1,2, \dots n \tag{8}$$

Then the equilibrium of system (7) is locally finite-time stable.
Lemma 5 [29] (finite-time stability of switched systems): Consider the class of switched systems described as

$$\dot{\boldsymbol{x}} = \boldsymbol{f}_\sigma(\boldsymbol{x}),\ \ \boldsymbol{f}_\sigma(0) = 0 \tag{9}$$

where $\boldsymbol{x} \in \mathbb{R}^n$, $\boldsymbol{x}(t_0) = \boldsymbol{x}_{\mathbf{0}}$.
Let Σ_f denotes the finite switching index set and assume that $\boldsymbol{f}_i \in F \triangleq \{f_j\}, j \in \Sigma_f \triangleq \{1,2, \dots, N_f\}$ is continuous with respect to $\boldsymbol{x}$ and the switching signal $\sigma_f \in \mathbb{R}_+ \times \mathbb{R}^n \to \Sigma_f$ is a piecewise constant function of time. If system (9) is asymptotically stable and $\dot{\boldsymbol{x}} = \boldsymbol{f}_i(\boldsymbol{x})$ for fixed $i \in \Sigma_f$ is finite-time stable, then the switched system (9) is finite-time stable.
Lemma 6 [31] (Barbalat's principle): Consider a Lyapunov function $\mathrm{V}(\boldsymbol{x}): \boldsymbol{D} \to \mathbb{R}$ with

1. $\mathrm{V}(\boldsymbol{x}) > 0$ and $\mathrm{V}(0) = 0$,
2. $\mathrm{V}(\boldsymbol{x}) \leq \mu \in \mathbb{R}^+$ (lower bounded)

It follows that

1. $\mathrm{V}(\boldsymbol{x})$ is strong if $\dot{\mathrm{V}}(\boldsymbol{x}) \leq -h(\boldsymbol{x}) \in \mathbb{R}^+$
2. $\mathrm{V}(\boldsymbol{x})$ is weak if $\dot{\mathrm{V}}(\boldsymbol{x}) \leq 0$
3. If $\ddot{\mathrm{V}}(\boldsymbol{x})$ is bounded, then $\lim_{t\to\infty} \left(\dot{\mathrm{V}}(\boldsymbol{x})\right) = 0$

Lemma 7: (Rayleigh quotient): Let $\boldsymbol{P}$ and $\boldsymbol{z}$ being a symmetric positive definite matrix and a nonzero vector, respectively. The corresponding Rayleigh quotient $R(\boldsymbol{P}, \boldsymbol{z})$ is bounded as follows

$$\lambda_{min}(\boldsymbol{P}) \leq R(\boldsymbol{P}, \boldsymbol{z}) = \frac{\boldsymbol{z}^T \boldsymbol{P} \boldsymbol{z}}{\boldsymbol{z}^T \boldsymbol{z}} \leq \lambda_{max}(\boldsymbol{P}) \tag{10}$$

where $\lambda_{min}(\boldsymbol{P})$, $\lambda_{max}(\boldsymbol{P})$ are the smallest and the largest eigenvalues of $\boldsymbol{P}$.

3. Satellite Attitude Synchronization

Consider the case of a group of n satellites labelled $'1,..n'$ and a virtual leader labelled $'0'$. Since the SFF control aims to enforce satellites agents to track desired dynamics (virtual leader states), we define $\boldsymbol{q}_d$ and $\boldsymbol{\omega}_d$ as the desired states for each agent relative to the inertial frame $\mathcal{F}_0$.

Definition 1: Assuming that the SFF attitude is described by Eq. (1), the finite-time closed-loop system stability and attitude synchronization can be achieved if, for any initial values of the system states, there exists a synchronization time $T \in [0, +\infty)$ such that the solution of Eq. (1) satisfies

$$\lim_{t\to T}(\boldsymbol{q}_i - \boldsymbol{q}_0) = 0, \lim_{t\to T}(\boldsymbol{\omega}_i - \boldsymbol{\omega}_0) = 0 \qquad (11a)$$

$$\boldsymbol{q}_i = \boldsymbol{q}_0, \quad \boldsymbol{\omega}_i = \boldsymbol{\omega}_0, \quad \forall t \geq T, i \in \mathcal{N} \qquad (11b)$$

The synchronization time T depends on the initial values of the system states

$$\boldsymbol{x}_i(t_0) = \boldsymbol{x}_{i0}, \quad \boldsymbol{\omega}_i(t_0) = \boldsymbol{\omega}_{i0}, \quad \forall\, i \in \mathcal{N} \qquad (12)$$

3.1 FSS Attitude Synchronization with Fixed Network

Consider the system described by Eq. (1) with fixed network topologies where the interconnection among the nodes (satellites) remains unchanged over time. To achieve the finite-time synchronization of the i-th satellite in the formation, we choose the following control law

$$\begin{aligned}\boldsymbol{\tau}_i = {} & \boldsymbol{\omega}_i^{\times}\boldsymbol{J}_i\boldsymbol{\omega}_i - \\ & k_1\boldsymbol{J}_i\left\{\sum_{j\in\mathcal{N}}\left[a_{ij}(\boldsymbol{q}_i-\boldsymbol{q}_j)\right]^{\alpha} + [b_i(\boldsymbol{q}_i-\boldsymbol{q}_0)]^{\alpha}\right\} - \\ & k_2\boldsymbol{J}_i\left\{\sum_{j\in\mathcal{N}}\left[a_{ij}(\boldsymbol{\omega}_i-\boldsymbol{\omega}_j)\right]^{\beta} + [b_i(\boldsymbol{\omega}_i-\boldsymbol{\omega}_0)]^{\beta}\right\}\end{aligned} \qquad (13)$$

where $k_1, k_2 > 0$ are the control gain, with $0 < \alpha < 1, \beta \geq 1$ and the skew-symmetric matrix $\boldsymbol{\omega}_i^{\times}(\boldsymbol{\omega})$ is defined as

$$\boldsymbol{\omega}_i^{\times} = \begin{pmatrix} 0 & -\omega_z & \omega_y \\ \omega_z & 0 & -\omega_x \\ -\omega_y & \omega_x & 0 \end{pmatrix} \qquad (14)$$

For each i-th satellite, the first term in the control protocol (13) describes the compensation for the nonlinear dynamics in Eq. (1), the second term penalizes errors in the attitude synchronization, and the third term ensures the finite-time convergence of the angular velocity towards the leader one.

Theorem 1: Suppose that assumptions 1-3 hold. Then, the finite-time synchronization of the SFF in Eq. (1) around the attitude of the leader according to the agreement (11) can be achieved by the local torque control law (13) if, for $k_1, k_2 > 0$, the parameters α and β are selected such that $0 < \alpha < 1$ and $\beta = 2\alpha/(1+\alpha)$.

Proof: Define $\widehat{\boldsymbol{q}}_i = \boldsymbol{q}_i - \boldsymbol{q}_0, \widehat{\boldsymbol{\omega}}_i = \boldsymbol{\omega}_i - \boldsymbol{\omega}_0, \forall i \in \mathcal{N}$ to be the tracking quaternion and angular velocity errors, respectively. Then we have from Eqs. (1) and (13)

$$\begin{aligned}\dot{\widehat{\boldsymbol{q}}}_i = {} & -\frac{1}{2}\widehat{\boldsymbol{\omega}}_i \times \widehat{\boldsymbol{q}}_i + \frac{1}{2}q_{0i}\widehat{\boldsymbol{\omega}}_i \\ \dot{\widehat{\boldsymbol{\omega}}}_i = {} & -J_i^{-1}\widehat{\boldsymbol{\omega}}_i \times (J_i\widehat{\boldsymbol{\omega}}_i) + \widehat{\boldsymbol{\omega}}_i^{\times}\boldsymbol{J}_i\widehat{\boldsymbol{\omega}}_i - \\ & -k_1\boldsymbol{J}_i\left\{\sum_{j\in\mathcal{N}}\left[a_{ij}(\widehat{\boldsymbol{q}}_i-\widehat{\boldsymbol{q}}_j)\right]^{\alpha} + [b_i(\widehat{\boldsymbol{q}}_i)]^{\alpha}\right\} \\ & - k_2\boldsymbol{J}_i\left\{\sum_{j\in\mathcal{N}}\left[a_{ij}(\widehat{\boldsymbol{\omega}}_i-\widehat{\boldsymbol{\omega}}_j)\right]^{\beta} + [b_i(\widehat{\boldsymbol{\omega}}_i)]^{\beta}\right\}\end{aligned} \qquad (15)$$

The objective here is to prove that the consensus (11) can be achieved within a finite-time synchronization T. To do so, consider a positive definite Lyapunov function candidate as

$$V = V_1 + V_2 \qquad (16a)$$

where

$$\begin{aligned}V_1 = {} & \frac{1}{2}\sum_{i=1}^{n}\sum_{j=1}^{n}\int_0^{\widehat{q}_i-\widehat{q}_j} k_1\boldsymbol{J}_i\left[a_{ij}(\widehat{\boldsymbol{q}}_i-\widehat{\boldsymbol{q}}_j)\right]^{\alpha} ds \\ & + \sum_{1=1}^{n}\int_0^{\widehat{q}_i} k_1\boldsymbol{J}_i[b_i\widehat{\boldsymbol{q}}_i]^{\alpha} ds\end{aligned} \qquad (16b)$$

$$V_2 = \frac{1}{2}\sum_{i=1}^{n}\widehat{\boldsymbol{\omega}}_i^2 \qquad (16c)$$

Tacking the time derivative of V along the trajectories of system (15)

$$\begin{aligned}\dot{V} = {} & \frac{1}{2}\sum_{i=1}^{n}\sum_{j\in\bar{\mathcal{N}}} k_1\boldsymbol{J}_i\left[a_{ij}(\widehat{\boldsymbol{q}}_i-\widehat{\boldsymbol{q}}_j)\right]^{\alpha}(\widehat{\boldsymbol{\omega}}_i-\widehat{\boldsymbol{\omega}}_j) \\ & + \sum_{i=1}^{n} k_1\boldsymbol{J}_i b_i(\widehat{\boldsymbol{q}}_i)^{\alpha}\widehat{\boldsymbol{\omega}}_i + \sum_{i=1}^{n}\widehat{\boldsymbol{\omega}}_i^T[-J_i^{-1}\widehat{\boldsymbol{\omega}}_i \times (J_i\widehat{\boldsymbol{\omega}}_i) + \widehat{\boldsymbol{\omega}}_i^{\times}\boldsymbol{J}_i\widehat{\boldsymbol{\omega}}_i \\ & + \sum_{i=1}^{n}\widehat{\boldsymbol{\omega}}_i^T[-J_i^{-1}\widehat{\boldsymbol{\omega}}_i \times (J_i\widehat{\boldsymbol{\omega}}_i) + \widehat{\boldsymbol{\omega}}_i^{\times}\boldsymbol{J}_i\widehat{\boldsymbol{\omega}}_i \\ & -k_1\boldsymbol{J}_i\left\{\sum_{j\in\mathcal{N}}\left[a_{ij}(\widehat{\boldsymbol{q}}_i-\widehat{\boldsymbol{q}}_j)\right]^{\alpha} + [b_i(\widehat{\boldsymbol{q}}_i)]^{\alpha}\right\} \\ & - k_2\boldsymbol{J}_i\left\{\sum_{j\in\mathcal{N}}\left[a_{ij}(\widehat{\boldsymbol{\omega}}_i-\widehat{\boldsymbol{\omega}}_j)\right]^{\beta} + [b_i(\widehat{\boldsymbol{\omega}}_i)]^{\beta}\right\}\Bigg]\end{aligned} \qquad (17)$$

$$
\begin{aligned}
&= \sum_{i=1}^{n} \widehat{\boldsymbol{\omega}}_i^T [-\boldsymbol{J}_i^{-1} \widehat{\boldsymbol{\omega}}_i \times (\boldsymbol{J}_i \widehat{\boldsymbol{\omega}}_i) + \widehat{\boldsymbol{\omega}}_i^{\times} \boldsymbol{J}_i \widehat{\boldsymbol{\omega}}_i] \\
&- k_2 \sum_{i=1}^{n} \widehat{\boldsymbol{\omega}}_i^T \; \boldsymbol{J}_i \left\{ \sum_{j \in \mathcal{N}} \left[a_{ij} \left(\widehat{\boldsymbol{\omega}}_i - \widehat{\boldsymbol{\omega}}_j \right) \right]^{\beta} + [b_i (\widehat{\boldsymbol{\omega}}_i)]^{\beta} \right\} \Bigg] \\
&= \sum_{i=1}^{n} \widehat{\boldsymbol{\omega}}_i^T [-\boldsymbol{J}_i^{-1} \widehat{\boldsymbol{\omega}}_i \times (\boldsymbol{J}_i \widehat{\boldsymbol{\omega}}_i) + \widehat{\boldsymbol{\omega}}_i^{\times} \boldsymbol{J}_i \widehat{\boldsymbol{\omega}}_i] \\
&- \frac{k_2}{2} \sum_{i=1}^{n} \sum_{\in \mathcal{N}} \boldsymbol{J}_i \left(\widehat{\boldsymbol{\omega}}_i - \widehat{\boldsymbol{\omega}}_j \right) \left[a_{ij} \left(\widehat{\boldsymbol{\omega}}_i - \widehat{\boldsymbol{\omega}}_j \right) \right]^{\beta} \\
&- \sum_{i=1}^{n} \widehat{\boldsymbol{\omega}}_i^T \boldsymbol{J}_i [b_i (\widehat{\boldsymbol{\omega}}_i)]^{\beta}
\end{aligned}
$$

For $k_2 > 0$

$$
\dot{V} < \sum_{i=1}^{n} \widehat{\boldsymbol{\omega}}_i^T [-\boldsymbol{J}_i^{-1} \widehat{\boldsymbol{\omega}}_i \times (\boldsymbol{J}_i \widehat{\boldsymbol{\omega}}_i) + \widehat{\boldsymbol{\omega}}_i^{\times} \boldsymbol{J}_i \widehat{\boldsymbol{\omega}}_i] \tag{18}
$$

Since $\widehat{\boldsymbol{\omega}}_i \times (\boldsymbol{J}_i \widehat{\boldsymbol{\omega}}_i) = \widehat{\boldsymbol{\omega}}_i^{\times} \boldsymbol{J}_i \widehat{\boldsymbol{\omega}}_i$, it results that

$$
\begin{aligned}
\dot{V} &\leq \widehat{\boldsymbol{\omega}}_i^T (\boldsymbol{I} - \boldsymbol{J}_i^{-1}) \widehat{\boldsymbol{\omega}}_i^{\times} \boldsymbol{J}_i \widehat{\boldsymbol{\omega}}_i \\
&\leq 0
\end{aligned} \tag{20}
$$

To prove that the agreement (11) holds for each agent, we consider the case $\dot{V} = 0$

$$
\begin{aligned}
&\sum_{i=1}^{n} \widehat{\boldsymbol{\omega}}_i^T [-\boldsymbol{J}_i^{-1} \widehat{\boldsymbol{\omega}}_i \times (\boldsymbol{J}_i \widehat{\boldsymbol{\omega}}_i) + \widehat{\boldsymbol{\omega}}_i^{\times} \boldsymbol{J}_i \widehat{\boldsymbol{\omega}}_i] \\
&- \frac{k_2}{2} \sum_{i=1}^{n} \sum_{\in \mathcal{N}} \boldsymbol{J}_i \left(\widehat{\boldsymbol{\omega}}_i - \widehat{\boldsymbol{\omega}}_j \right) \left[a_{ij} \left(\widehat{\boldsymbol{\omega}}_i - \widehat{\boldsymbol{\omega}}_j \right) \right]^{\beta} \\
&- \sum_{i=1}^{n} \widehat{\boldsymbol{\omega}}_i^T \boldsymbol{J}_i [b_i (\widehat{\boldsymbol{\omega}}_i)]^{\beta} = 0
\end{aligned} \tag{21}
$$

The condition (21) can hold if and only if $\widehat{\boldsymbol{\omega}}_i = \widehat{\boldsymbol{\omega}}_j = 0$ which implies $\dot{\widehat{\boldsymbol{\omega}}}_i = 0$. From Eq. (15), it follows

$$
\sum_{j \in \mathcal{N}} \left[a_{ij} \left(\widehat{\boldsymbol{q}}_i - \widehat{\boldsymbol{q}}_j \right) \right]^{\alpha} + [b_i (\widehat{\boldsymbol{q}}_i)]^{\alpha} = 0 \tag{22}
$$

Equality (22) implies that $\widehat{\boldsymbol{q}}_i = \widehat{\boldsymbol{q}}_j = 0 \;\; \forall i, j \in \mathcal{N}$. From Lemma 2, $\boldsymbol{q}_i - \boldsymbol{q}_0 \to 0, \boldsymbol{\omega}_i - \boldsymbol{\omega}_0 \to 0, \forall i \in \mathcal{N}$, as $t \to \infty$. Define the homogeneity degree of system (15) as $p = \alpha - 1 < 0$, according to Lemma 3 the equilibrium of system (15) is globally asymptotically stable with local finite-time convergence. It results that the origin is a globally finite-time stable equilibrium of system (15) and the consensus (11) is reached in finite-time. This completes the proof.

3.2 SFF Synchronization with Switching Network

Consider the case of networked systems with switching communication topologies. Let $G_s = \{\mathcal{V}, \mathcal{E}, \boldsymbol{\mathcal{A}}_{\sigma(t)}\}$ denotes the finite set of all possible topologies, $\mathcal{M} = \{1,2, \dots, M\}$ denotes the index set, and M denotes the number of switching topologies. We define a switching signal $\sigma(t): R^{+} \to \mathcal{M}$ and a switching sequence of bounded non-overlapping time intervals $[t_s, t_{s+1})$. The control objective is now to reach following switched state consensus in finite-time.

$$
\begin{aligned}
\lim_{t \in [\boldsymbol{t_s}, \boldsymbol{t_{s+1}})} (\boldsymbol{q}_i - \boldsymbol{q}_0) = 0 \\
\lim_{t \in [\boldsymbol{t_s}, \boldsymbol{t_{s+1}})} (\boldsymbol{\omega}_i - \boldsymbol{\omega}_0) = 0
\end{aligned} \tag{23}
$$

where $t \in [t_s, t_{s+1})$, $t_{s+1} - t_s = \tau > 0$ is the dwell period and $k = 0,1, \dots, M$. We define a_{ij}^s and b_i^s as agent-to-agent and agent-to-leader adjacency weights, respectively.

Theorem 2: *Suppose that assumption 4 holds. Then for a switching SFF with a dwelling period τ, the finite-time synchronization of the formation can be achieved by the following individual satellite torques*

$$
\begin{aligned}
\boldsymbol{\tau}_i = \; &\boldsymbol{\omega}_i^{\times}(t) \boldsymbol{J}_i \boldsymbol{\omega}_i(t) - k_1 \boldsymbol{J}_i \sum_{j \in \mathcal{N}} \left[a_{ij}^s \left(\boldsymbol{q}_i - \boldsymbol{q}_j \right) \right]^{\alpha} \\
&- k_2 \boldsymbol{J}_i \sum_{j \in \mathcal{N}} \left[a_{ij}^s \left(\boldsymbol{\omega}_i - \boldsymbol{\omega}_j \right) \right]^{\beta} - k_1 \boldsymbol{J}_i [b_i^s (\boldsymbol{q}_i - \boldsymbol{q}_0)]^{\alpha} \\
&- k_2 \boldsymbol{J}_i [b_i^s (\boldsymbol{\omega}_i - \boldsymbol{\omega}_0)]^{\beta}
\end{aligned} \tag{24}
$$

Proof: Under switching communication topologies, system (15) can be written as

$$
\begin{aligned}
\dot{\widehat{\boldsymbol{q}}}_i = \; &-\frac{1}{2} \widehat{\boldsymbol{\omega}}_i \times \widehat{\boldsymbol{q}}_i + \frac{1}{2} q_{0i} \widehat{\boldsymbol{\omega}}_i \\
\dot{\widehat{\boldsymbol{\omega}}}_i = \; &-J_i^{-1} \widehat{\boldsymbol{\omega}}_i \times (J_i \widehat{\boldsymbol{\omega}}_i) + \widehat{\boldsymbol{\omega}}_i^{\times} \boldsymbol{J}_i \widehat{\boldsymbol{\omega}}_i - \\
&- k_1 \boldsymbol{J}_i \left\{ \sum_{j \in \mathcal{N}} \left[a_{ij}^k \left(\widehat{\boldsymbol{q}}_i - \widehat{\boldsymbol{q}}_j \right) \right]^{\alpha} + \left[b_i^k (\widehat{\boldsymbol{q}}_i) \right]^{\alpha} \right\} \\
&- k_2 \boldsymbol{J}_i \left\{ \sum_{j \in \mathcal{N}} \left[a_{ij}^k \left(\widehat{\boldsymbol{\omega}}_i - \widehat{\boldsymbol{\omega}}_j \right) \right]^{\beta} + \left[b_i^k (\widehat{\boldsymbol{\omega}}_i) \right]^{\beta} \right\}
\end{aligned} \tag{25}
$$

For $t \in [t_k, t_{k+1})$ and $s \in \mathcal{M}$, a Lyapunov candidature function is chosen as

$$
\begin{aligned}
V_1 = &\frac{1}{2} \sum_{i=1}^{n} \sum_{j=1}^{n} \int_0^{\widehat{q}_i - \widehat{q}_j} k_1 \boldsymbol{J}_i \left[a_{ij}^s \left(\widehat{\boldsymbol{q}}_i - \widehat{\boldsymbol{q}}_j \right) \right]^{\alpha} ds \\
&+ \sum_{1=1}^{n} \int_0^{\widehat{q}_i} k_1 \boldsymbol{J}_i [b_i^s \widehat{\boldsymbol{q}}_i]^{\alpha} ds + \frac{1}{2} \sum_{i=1}^{n} \widehat{\boldsymbol{\omega}}_i^2
\end{aligned} \tag{26}
$$

As in the proof of theorem 1, a condition like (8) can be written as

$$\sum_{i=1}^{n} \widehat{\boldsymbol{\omega}}_i^T[-\boldsymbol{J}_i^{-1}\widehat{\boldsymbol{\omega}}_i \times (\boldsymbol{J}_i\widehat{\boldsymbol{\omega}}_i)+\widehat{\boldsymbol{\omega}}_i^{\times}\boldsymbol{J}_i\widehat{\boldsymbol{\omega}}_i]$$
$$-\frac{k_2}{2}\sum_{i=1}^{n}\sum_{\in\mathcal{N}} \boldsymbol{J}_i(\widehat{\boldsymbol{\omega}}_i - \widehat{\boldsymbol{\omega}}_j)\left[a_{ij}^s(\widehat{\boldsymbol{\omega}}_i - \widehat{\boldsymbol{\omega}}_j)\right]^{\beta} \quad (27)$$
$$-\sum_{i=1}^{n} \widehat{\boldsymbol{\omega}}_i^T\boldsymbol{J}_i[b_i^s(\widehat{\boldsymbol{\omega}}_i)]^{\beta} = 0$$

The new condition (27) is valid, if and only if, $\widehat{\boldsymbol{\omega}}_i = \widehat{\boldsymbol{\omega}}_j = 0$ which implies $\dot{\widehat{\boldsymbol{\omega}}}_i = 0$ and

$$\sum_{j\in\mathcal{N}} \left[a_{ij}^s(\widehat{\boldsymbol{q}}_i - \widehat{\boldsymbol{q}}_j)\right]^{\alpha} + [b_i^s(\widehat{\boldsymbol{q}}_i)]^{\alpha} = 0 \quad (28)$$

It results from conditions (27) and (28) that, $\forall t \in [t_s, t_{s+1})$ and $\forall \sigma(t) = m \in \mathcal{M}$, the agreement (23) holds, which implies that $\boldsymbol{q}_i - \boldsymbol{q}_0 \to 0, \boldsymbol{\omega}_i - \boldsymbol{\omega}_0 \to 0, \forall i \in \mathcal{N}$. Consequently, the origin is a finite-time stable equilibrium of system (25) and according to Lemma 3, the system (25) is finite-time convergent. *This completes the proof.*

4. Finite-time SFF control design with HOSM Estimator

In this section, a high-order sliding mode angular velocity estimator is designed based on the super-twisting algorithm. The distributed estimator allows satellites to estimate accurately the desired angular velocity in the presence of disturbances and in case of loss of communication among SFF agents or with the leader. The distributed sliding mode observer is obtained, for each agent *'i'*, as follows

$$\begin{cases} \dot{\hat{\boldsymbol{z}}}_i = -\lambda_1\|\boldsymbol{\sigma}_i\|_2^{1/2} sign(\boldsymbol{\sigma}_i) + \boldsymbol{\varphi}_i \\ \dot{\boldsymbol{\varphi}}_i = -\lambda_2 sign(\boldsymbol{\sigma}_i) \end{cases} \quad (29)$$

with $\boldsymbol{z}_i, \boldsymbol{\varphi}_i$ being the observer states and $\boldsymbol{\sigma}_i$ the sliding mode surface defined as

$$\boldsymbol{\sigma}_i = \left\{\sum_{j\in\mathcal{N}} a_{ij}(\widehat{\boldsymbol{\omega}}_i - \widehat{\boldsymbol{\omega}}_j) + b_i(\widehat{\boldsymbol{\omega}}_i - \boldsymbol{\omega}_d)\right\} \quad (30)$$

$\lambda_1, \lambda_1 \in \mathbb{R}^+$ are the observer parameters. Considering $\widehat{\boldsymbol{\omega}}_i = \boldsymbol{Q}_i\boldsymbol{z}_i$ as the angular velocity estimator, the distributed control law (13) is replaced by the following control law

$$\boldsymbol{\tau}_i = \boldsymbol{\omega}_i^{\times}\boldsymbol{J}_i\widehat{\boldsymbol{\omega}}_i - k_1\boldsymbol{J}_i\sum_{j\in\mathcal{N}}\left[a_{ij}^s(\boldsymbol{q}_i - \boldsymbol{q}_j)\right]^{\alpha}$$
$$-k_1\boldsymbol{J}_i[b_i^s(\boldsymbol{q}_i - \boldsymbol{q}_0)]^{\alpha} - k_2\boldsymbol{J}_i\boldsymbol{Q}_i\dot{\widehat{\boldsymbol{\omega}}}_i^{\beta} \quad (31)$$

Theorem 3: *Assume that the graph G is undirected and at least one $b_i > 0$. The distributed control law (31) ensures that $\lim_{t\to T}(\boldsymbol{q}_i - \boldsymbol{q}_j) = 0$ and $\lim_{t\to T}(\widehat{\boldsymbol{\omega}}_i) = \lim_{t\to T}(\widehat{\boldsymbol{\omega}}_j) = \boldsymbol{\omega}_d$ in finite-time, if there exists a pair of parameters $\lambda_1, \lambda_2 > 0$ that make the following matrices $\boldsymbol{P}$ and $\boldsymbol{Q}$ positive definite symmetric,*

$$\boldsymbol{P} = \frac{1}{2}\begin{bmatrix} 4\lambda_2 + \lambda_1^2 & -\lambda_1 \\ -\lambda_1 & 2 \end{bmatrix}, \quad \boldsymbol{Q} = \frac{\lambda_1}{2}\begin{bmatrix} 2\lambda_2 + \lambda_1^2 & -\lambda_1 \\ -\lambda_1 & 1 \end{bmatrix}$$

Proof. To prove that the super-twisting estimator (29) can guarantee the finite-time convergence of $\widehat{\boldsymbol{\omega}}_i \to \boldsymbol{\omega}_d$, we define a vector $\boldsymbol{\xi}_i = \left[\|\boldsymbol{\sigma}_i\|_2^{1/2} \quad \|\boldsymbol{\varphi}_i\|_2\right]^T$, $i = \{1, \dots, n\}$. Consider, for each agent $'i'$, a quadratic form V_i corresponding to $\boldsymbol{P}$ and being a Lyapunov function candidate

$$\mathrm{V_i} = \boldsymbol{\xi}_\mathbf{i}^\mathrm{T}\mathbf{P}\boldsymbol{\xi}_\mathbf{i} \quad (32)$$

From Lemma 7, it results that the functions V_i $(i = 1, \dots, n)$ are bounded by

$$\lambda_{\min}(\mathbf{P})\,\|\boldsymbol{\xi}_\mathbf{i}\|_2^2 \le \mathrm{V_i} \le \lambda_{\max}(\mathbf{P})\,\|\boldsymbol{\xi}_\mathbf{i}\|_2^2 \quad (33)$$

One can find that the time derivatives of the functions $\boldsymbol{\xi}_i$ and V_i are given as follows

$$\dot{\boldsymbol{\xi}}_i = \frac{1}{|\xi_{i,1}|}\left[\left(-\frac{\lambda_1}{2}\xi_{i,1} + \frac{1}{2}\xi_{i,2}\right) \quad \left(-\lambda_2\xi_{i,1} + |\xi_{i,1}|\right)\right] \quad (34)$$

$$\dot{\mathrm{V}}_\mathrm{i} = \frac{-1}{|\xi_{\mathrm{i},1}|^{1/2}}\boldsymbol{\xi}_\mathbf{i}^\mathrm{T}\mathbf{Q}\boldsymbol{\xi}_\mathbf{i} \quad (35)$$

It follows that

$$\dot{\mathrm{V}}_\mathrm{i} \le \frac{-\lambda_{\min}(\mathbf{Q})}{|\xi_{\mathrm{i},1}|^{1/2}}\|\boldsymbol{\xi}_\mathbf{i}\|_2^2 \le \frac{-1}{|\xi_{\mathrm{i},1}|^{1/2}}\frac{\lambda_{\min}(\mathbf{Q})}{\lambda_{\max}(\mathbf{P})}\|\boldsymbol{\xi}_\mathbf{i}\|_2^2 \quad (36)$$

where $\|\boldsymbol{\xi}_i\|_2^2 = \|\boldsymbol{\sigma}_i\|_2 + \|\boldsymbol{\varphi}_i\|_2^2$ is the Euclidian norm of $\dot{\boldsymbol{\xi}}_i$ and $\lambda_{min}(\boldsymbol{Q}), \lambda_{max}(\boldsymbol{P})$ are the minimum and maximum eigenvalues of the matrices $\boldsymbol{Q}$ and $\boldsymbol{P}$, respectively.

Knowing that $|\xi_{i,1}|^{1/2} \le \|\boldsymbol{\xi}_i\|_2$ and using the inequality (33), it follows that

$$|\xi_{\mathrm{i},1}|^{1/2} \le \frac{\mathrm{V_i}^{1/2}(\boldsymbol{\xi}_\mathbf{i})}{\lambda_{\min}^{1/2}(\mathbf{P})} \quad (37)$$

$$\dot{\mathrm{V}}_\mathrm{i} \le -\eta \mathrm{V_i}^{1/2}(\boldsymbol{\xi}_\mathbf{i}) \quad (38)$$

with

$$\eta = \frac{\lambda_{\min}^{1/2}(\mathbf{P})\lambda_{\min}(\mathbf{Q})}{\lambda_{\max}(\mathbf{P})} \quad (39)$$

End of proof.

5. Numerical Simulations

In this section, numerical examples are given to illustrate the obtained theoretical results and demonstrate the effectiveness and performance of the proposed distributed SFF attitude synchronization protocols. The different torque control laws and the angular velocity estimator are simulated to achieve finite-time attitude synchronization of a given SFF. The satellites orbit under the undirected graph $G_k, k = 1, .., 4$ as shown in Fig. 1.

For illustration, two scenarios are considered. In the first scenario, the control laws (13) and (24) are us to achieve unperturbed SFF attitude synchronization in finite-time. In the second scenario, the observer-controller scheme given by Eqs. (29) and (31) is used to enable the formation satellites to track a desired time-varying angular velocity in the presence of external disturbances and under switched communication topology.

For fair comparison, the data of the three-satellite SFF given in [11] is used in the simulations. The case where the three satellites orbit with a switching communication topology composed of four digraphs G_1-G_4 as shown in Fig 1 is considered. For simplicity, the adjacency matrix elements are 0 or 1. Table 1 gives the SFF parameters and initial conditions.

Table 1 Simulation parameters

Index	Inertiel matrix $\boldsymbol{J}$ (kg/m^2)	Initial $\boldsymbol{q}(0)$	Initial $\boldsymbol{\omega}(0)$ (rad/s)
1	$diag\{24.31,24.37,23.64\}$	$[0.8986,0.4,-0.1,0.15]^T$	$[0.13,-0.15,0.1]^T$
2	$diag\{20.25,20.33,20.66\}$	$[0.8888,-0.2,0.1,0.40]^T$	$[0.11,0.16,-0.08]^T$
3	$diag\{30.35,30.17,30.61\}$	$[0.8426,-0.4,-0.2,0.3]^T$	$[-0.1,0.12,-0.13]^T$

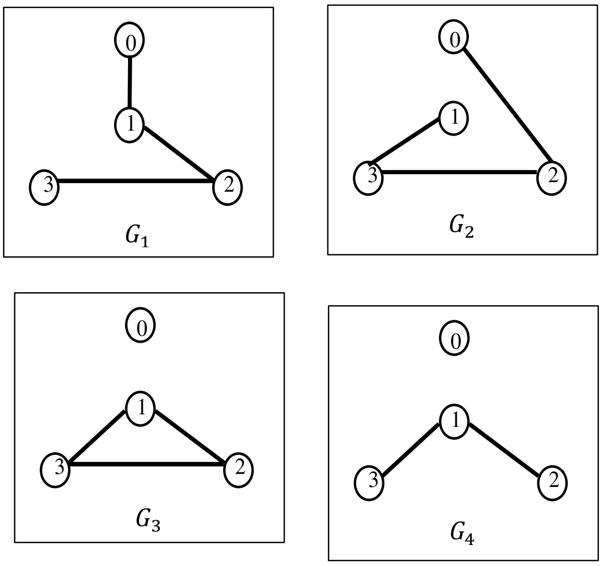

Fig. 1 Four diagraphs $\mathrm{G}_1-\mathrm{G}_4$ communication topology of three-satellite SFF

Scenario 1: The attitude of the satellites in formation is enforced to achieve the unperturbed consensus $\mathbf{q}_\mathrm{i} \rightarrow \mathbf{q}_\mathrm{d} = [1,0,0,0]^\mathrm{T}, \boldsymbol{\omega}_\mathrm{i} \rightarrow \boldsymbol{\omega}_\mathrm{d} = [0,0,0]^\mathrm{T}$ in finite-time. The parameters of the controller given by Eq. (24) are given as $a = 0.85$, $\mathrm{b} = 2\mathrm{a}/(1+\mathrm{a}) = 0.92$, $\mathrm{k}_1 = 1.25, \mathrm{k}_2 = 1.5$ and dwell time $\tau = 20\mathrm{s}$. The attitude and angular velocity tracking errors for the three satellites ($i = 1,2,3$) and their required control inputs (torques) are shown in Figs. 2,3,4, respectively. Figure 2 shows that the synchronization occurs in approximately 20 s.

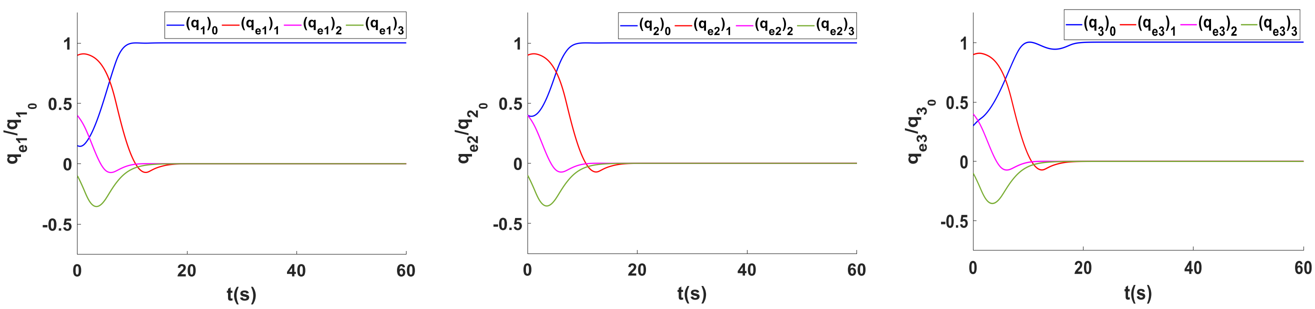

Fig. 2 Attitude tracking errors for SFF satellites with distributed controller (24)

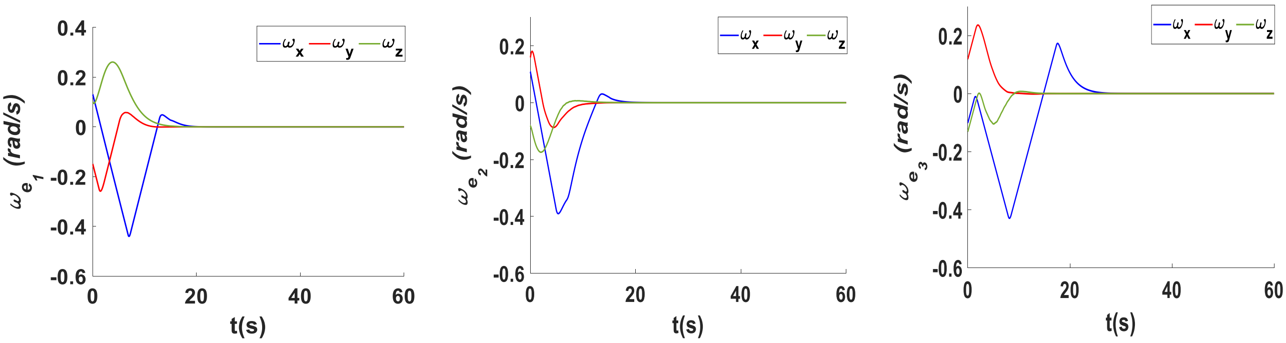

Fig. 3 Angular velocity tracking for SFF satellites with distributed controller (24)

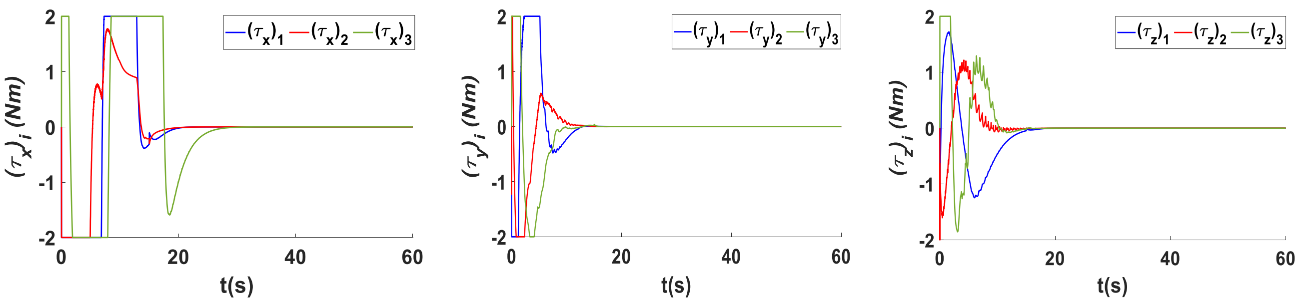

Fig. 4 Control inputs(torques) for SFF satellites with distributed controller (24)

Scenario 2: The observer-controller scheme given by Eqs. (29) and (31) is used to enable the satellites tracking a desired time-varying angular velocity $\boldsymbol{\omega}_d = 1/10[\sin(t/40), -\sin(t/50), -\cos(t/60)]^T (rad/s)$ in the presence of an external disturbance torque due to the orbital motion $\boldsymbol{d}_i = \boldsymbol{d} = [-1.025, \;\; 6.248, \;\; -2.415]^T \times 10^{-1}\, Nm.$ The control parameters are selected as $\alpha = 0.15$, $\beta = 0.26$, $k_1 = k_2 = 0.25$, $\lambda_1 = \lambda_2 = 0.5$ and dwell time $\tau = 15s$. Figs. 5,6 show the relative angular velocity errors $\boldsymbol{\omega}_{ij} = \boldsymbol{\omega}_i - \boldsymbol{\omega}_j$ and control torques, respectively. The SFF attitude synchronization accuracy is determined using the relative attitude errors $\overline{\boldsymbol{q}}_{ij} = \overline{\boldsymbol{q}}_j^* \overline{\boldsymbol{q}}_i$ for the three satellites. As shown in Fig. 7, a threshold of 10^{-9} occurs at 22 s. Figure 8 depicts the attitude tracking path for the three satellites using the observer-controller scheme (29)-(31).

The main contribution of the proposed control scheme is twofold. First, both controllers (24) and (31) enable finite-time SFF consensus, despite satellite-to-satellite or satellite-to-leader communication losses. It is worth noting that finite-time formation control under loss of communication is highly recommended for performance improvement rather than asymptotic formation control. Second, the controller (24) conjointly with the observer (29) provide more stable and chattering free SFF attitude tracking as compared to relevant recent works (e.g., [11]).

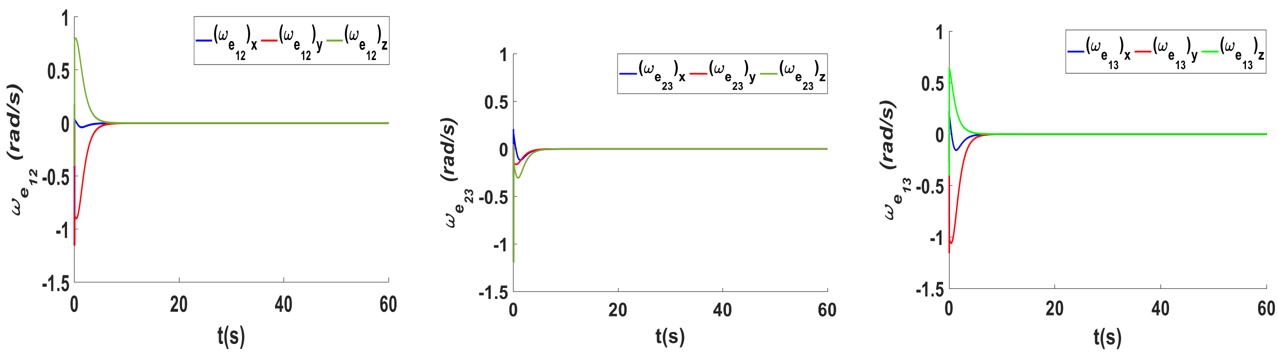

Fig. 5 Control inputs(torques) for SFF satellites with distributed controller (31)

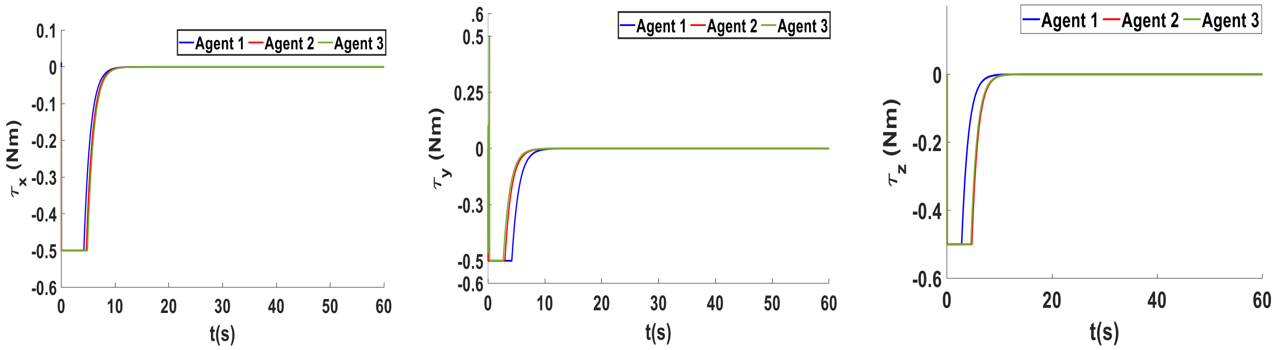

Fig. 6 Control inputs(torques) for SFF satellites with distributed controller (31)

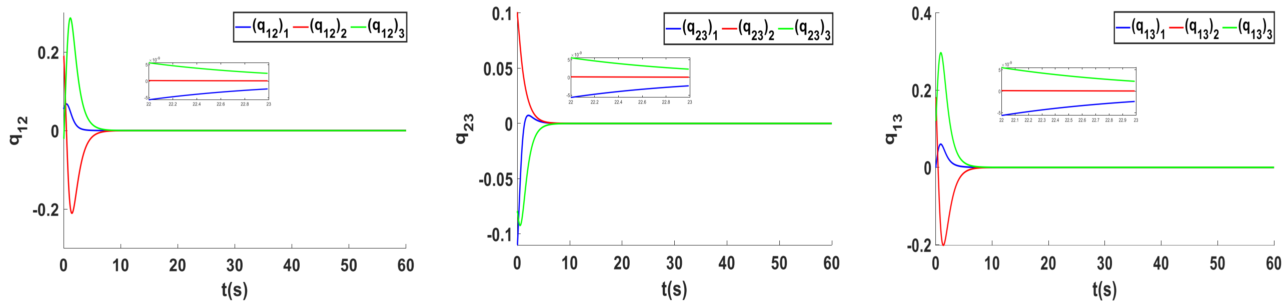

Fig. 7 Control inputs(torques) for SFF satellites with distributed controller (31)

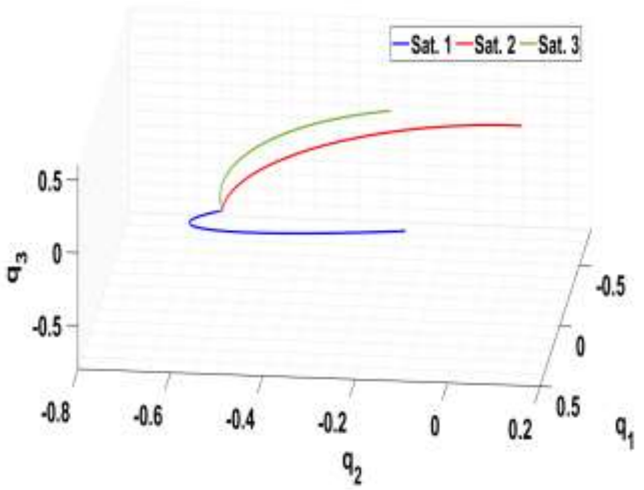

Fig. 7 Attitude tracking path for the three satellites of the SFF

6. Conclusion

The finite-time attitude synchronization problem for SFF under switching communication topology is investigated in this paper. First, SFF finite-time consensus problem under fixed and switching communication topologies was solved based upon graph and matrix theories, local finite-time convergence in homogeneous systems, and non-smooth LaSalle's invariance principle. Then, to reduce the number of communication links, supper-twisting sliding mode control theory was used to design a finite-time observer for estimating the desired angular velocity (i.e., leader velocity). Numerical simulations showed the outer performance and effectiveness of the proposed design.

Acknowledgment

This project was funded by the Deanship of Scientific Research (DSR), King Abdulaziz University, Jeddah, under grant No. (DF-484-135-1441). The authors, therefore, gratefully acknowledge DSR technical and financial support.

Compliance with ethical standards

Conflict of interest: The authors declare that they have no conflict of interest.

Data Availability Statement

Data sharing not applicable to this article as no datasets were generated or analysed during the current study

References

[1] Lee, D., Sanyal, A.K., & Butcher, E.A. (2015). Asymptotic tracking control for spacecraft formation flying with decentralized collision avoidance, Journal of Guidance, *Control and Dynamics*, **38**(4), 587–600.

[2] Shahbazi, B., Malekzadeh, M., & Koofigar, H.R. (2017). Robust constrained attitude control of spacecraft formation flying in the presence of disturbances. *IEEE Trans. Aerosp. Electron. Syst.* **53**(5), 2534–2543.
[3] Liu, G-P. & Zhang, S. (2018). A survey on formation control of small satellites, *Proceedings of the IEEE*, **106**(3), 440-457.
[4] Lee, D., Sanyal, A.K., & Butcher, E.A. (2014). Asymptotic tracking control for spacecraft formation flying with decentralized collision avoidance, *Journal of Guidance, Control, and Dynamics,* **38**(4), 587–600.
[5] Cai, H., & J Huang, J. (2016). Leader-following attitude consensus of multiple rigid body systems by attitude feedback control, *Automatica,* **69**, 87–92.
[6] Ren, W. (2010). Distributed cooperative attitude synchronization and tracking for multiple rigid bodies, *IEEE Trans. Control Syst. Technol*., **18**(2), 383–392.
[7] Cai H, & Huang, J. (2017). Leader-following attitude consensus of multiple uncertain spacecraft systems subject to external disturbance, *Int. J. Robust Nonlinear Control,* **27**(5), 742–760
[8] Zou, A., & Kumar, K.D. (2013). Quaternion-based distributed output feedback attitude coordination control for spacecraft formation flying. *Journal of Guidance, Control, and Dynamics,* **36**(2), 548–556.
[9] Scharf, D.P, Hadaegh, F.Y. & Ploen, S.R. (2003). A Survey of Spacecraft Formation Flying Guidance and Control (Part I): Guidance, *Proceeding of the 2003 American Control Conference,* 2976-2985.
[10] Scharf, D.P., Hadaegh, F.Y., & Ploen, S.R. (2004). A Survey of Spacecraft Formation Flying Guidance and Control (Part II): Control, *Proceeding of the 2004 American Control Conference*, 2976-2985.
[11] Zhou, J., & Hu, Q. (2013). Decentralized finite-time attitude synchronization control of satellite formation flying, *Journal of Guidance, Control, and Dynamics,* **36**(1), 185-195.
[12] Liu, X., Guo, Y., & Lu, P. (2014). Robust attitude coordination control for satellite formation with matched perturbations and measurement noises, *American Control Conference (ACC)***,** 3893-3898.
[13] Zhang, J., Hub, Q., & Xiec, W. (2017). Integral sliding mode-based attitude coordinated tracking for spacecraft formation with communication delays, *International Journal of Systems Science,* **48**(15), 3254-3266.
[14] Liu, H., Tian, Y., Lewis, F.L., Wan, Y., & Valavanis, K.P. (2019) Robust formation flying control for a team of satellites subject to nonlinearities and uncertainties, *Aerospace Science and Technology,* **95**(105455), 1-9.
[15] Jian, Z., Genting, Y., Qinglei, H., & Danwei, W. (2014). Finite-Time Attitude Synchronization for Spacecraft Formation Flying via Output Feedback, *Proceedings of the 33rd Chinese Control Conference,* 1638-1643.
[16] Huang Y., & Jia, Y. (2019). Adaptive finite-time distributed 6-DOF synchronization control for spacecraft formation without velocity measurement', *Nonlinear Dynamics,* **95**,2275–2291.
[17] Lin Z., Yingmin J. (2014). Decentralized adaptive attitude synchronization control for spacecraft formation using nonsingular fast terminal sliding mode, *Nonlinear Dynamics*, **78**, 2779–2794.
[18] Zhao, L., You, X., Sun, F., Liu, Z., & Yang, H. (2014). New tracking control method for synchronization of spacecraft formation with switching topologies, *Proceedings of the 33rd Chinese Control Conference,* 1208–1213.
[19] Yang, H., You, X., & Hua, Ch. (2016). Attitude tracking control for spacecraft formation with time-varying delays and switching topology, *Acta Astronautica*, **126**, 98-108.
[20] Zhang, J., Ye, D., Liu, M., & Sun., Z. (2017). Adaptive fuzzy finite-time control for spacecraft formation with communication delays and changing topologies, Journal of the Franklin Institute, **354,** 4377–4403.
[21] Lu, M. & Liu, L. (2020). Leader-following attitude consensus of multiple rigid spacecraft systems under switching networks, *IEEE Transactions on Automatic Control*, **65**(2), 839–845.
[22] Qinglei H., & Yongxia S. (2020). Event-based coordinated control of spacecraft formation flying under limited communication. *Nonlinear Dynamics*, **99**, 2139–2159.
[23] Yuan, Y., Wang, Y., & Guo, L. (2021). Sliding-mode-observer-based time-varying formation tracking for multispacecrafts subjected to switching topologies and time-delays, *IEEE Transactions on Automatic Control*, **66**(8), 3848-3855.
[24] Wen, J.T.Y., & Delgado, K.K. (1991). The Attitude Control Problem, *Institute of Electrical and Electronics Engineers Transactions on Automatic Control*, **36**(10), 1148–1162.
[25] Horn, R.A., Johnson, C.R. (1985). *Matrix Analysis*, Cambridge University Press, Cambridge.
[26] Ren, W., & Beard, R.W. (2005). Consensus seeking in multiagent systems under dynamically changing interaction topologies. IEEE Transactions on Automation Control, **50**(5), 655–661.
[27] Royden, H.L. (1988). *Real Analysis*, Macmillan Publishing Company, New York.
[28] Rouche, N. Habets, P. & Laloy, M. (1977). *Stability theory by Lyapunov's direct method*. New York: Springer-Verlag.
[29] Rosier, L. (1992) Homogeneous Lyapunov function for homogeneous continuous vector field, *Syst. Control Lett.,* **9**, 467–473.
[30] Wang, X. Hong, Y. (2010). "Distributed finite-time χ-consensus algorithms for multi-agent systems with variable coupling topology, *J. Syst Sci Complex*, **23**, 209–218.
[31] Slotine, J.J.E., & Li, W. (1991) *Applied Nonlinear Control*, Prentice Hall, Upper Saddle River, NJ.